

Article

Exploring the Efficiency of the q -Homotopy Analysis Transform Method for Solving a Fractional Initial Boundary Value Problem with a Nonlocal Condition

Said Mesloub * and Huda Alsaud

Mathematics Department, College of Science, King Saud University, P.O. Box 2455, Riyadh 11451, Saudi Arabia; halsaud@ksu.edu.sa

* Correspondence: mesloub@ksu.edu.sa

Abstract: This article employs the q -homotopy analysis transformation method (q -HATM) to numerically solve, subject to an integral condition, a fractional IBVP. The resulting numerical scheme is applied to solve, in which the exact solution is obtained, several test examples in order to illustrate its efficiency.

Keywords: q -homotopy; fractional derivative; Bessel operator; Laplace transform; auxiliary parameter; numerical scheme

MSC: 35D35; 35L20



Citation: Mesloub, S.; Alsaud, H. Exploring the Efficiency of the q -Homotopy Analysis Transform Method for Solving a Fractional Initial Boundary Value Problem with a Nonlocal Condition. *Axioms* **2023**, *12*, 790. <https://doi.org/10.3390/axioms12080790>

Academic Editor: Jorge E. Macías Díaz

Received: 12 June 2023

Revised: 9 August 2023

Accepted: 10 August 2023

Published: 15 August 2023



Copyright: © 2023 by the authors. Licensee MDPI, Basel, Switzerland. This article is an open access article distributed under the terms and conditions of the Creative Commons Attribution (CC BY) license (<https://creativecommons.org/licenses/by/4.0/>).

1. Introduction

During the last few decades, the topic of fractional calculus, as it provides more realistic mathematical models than those obtained by the classical technique for a great deal of phenomena in different disciplines, has captured the attention of mathematicians worldwide [1–12]. Unfortunately, obtaining the analytical form of the solution for fractional PDEs is more difficult than those obtained in integer PDEs. In the literature, there are several research articles that have been produced by many researchers, whereby different numerical techniques through which to handle the solution of fractional partial differential equation models (which appear in different applications and disciplines), were introduced, such as the Adomian decomposition method (ADM), the Laplace decomposition method (LDM), the homotopy analysis method (HAM), and the homotopy perturbation method (HPM) (see [13–21]).

The q -homotopy analysis method developed by El-Tavil and Huseen [22,23], where $q \in [0, \frac{1}{n}]$ and n are positive integers, is a modified version of the HAM introduced by Liao [24–28]. Another powerful numerical technique is the q -homotopy analysis transform method presented in [29–31]. This method combines the HAM and the Laplace transform method. The existence of the factor $(\frac{1}{n})^m$ in the power series solution that is generated by the q -HATM leads to a faster convergence than the original version of the homotopy analysis method.

Although these techniques have been widely used recently in handling linear and nonlinear problems, it is observed that the application of the ADM and the LDM both require decomposing the nonlinear terms into an infinite sum of polynomials, called Adomian polynomials, in the problem under consideration. The evaluation of these polynomials mostly requires tedious algebraic work. On the other hand, the HPM is viewed as a particular case of the HAM, which is achieved by setting the parameter $h = -1$. Thus, all results generated by the HPM can also be reproduced by the HAM as a particular case. Moreover, the HPM requires a good enough initial guess to ensure convergence, which is not necessary for the HAM as it involves the parameter h , which enables one

to control the convergence region. Also, for some strongly nonlinear problems, it fails to produce a convergent series solution; meanwhile, in HAM, the parameter h can be used to ensure the convergence of the power series solution for such problems. Thus, the HAM is a powerful technique that overcomes all the drawbacks of the abovementioned methods. In fact, the q -HATM is a modification of the HAM, and besides all the advantages inherited from the HAM, it involves the factor $(\frac{1}{n})^m$ in its series solutions, which accelerates the convergence.

Let us mention that, in the theory of the HAM, there is no theoretical technique that can be easily used to obtain the range of the auxiliary parameter h . But, in some limited cases (when a closed form of the series solution is obtained), these values can be determined by testing the convergence of this series. Unfortunately, most closed form series solutions are not obtained in practice, and the solutions are approximated by truncated ones. Therefore, the range of this parameter can be determined graphically using the h -curve, and is based on approximate truncated series solutions. Furthermore, the range on which the h -curve occurs is almost horizontal.

In this article, we will explore the efficiency of the q -HATM in solving, subject to a Dirichlet non-local condition of an integral type, a singular fractional IBVP. Namely, we will consider the numerical solution of the following fractional-order parabolic equation:

$$\left\{ \begin{array}{l} \mathcal{L}\eta = \mathcal{G}(x, t), (x, t) \in (0, 1) \times [0, T], \\ \ell\eta = \eta(x, 0) = w(x), 0 < x < 1, \\ \int_0^1 x \eta dx = 0, \eta(1, t) = 0, t \in (0, T), \end{array} \right. \tag{1}$$

where $\mathcal{G}(x, t)$ and $w(x)$ are known functions, and \mathcal{L} is an operator given by $\mathcal{L} = \partial_t^\nu - \frac{1}{x} \left(x \frac{\partial}{\partial x} \right)_x$, in which ∂_t^ν denotes the fractional derivative in the Caputo sense of order ν , which is defined by the following [7,8]:

$$\partial_t^\nu := \frac{\partial^\nu}{\partial t^\nu} \eta(x, t) = \begin{cases} \frac{1}{\Gamma(n-\nu)} \int_0^t \frac{\partial^n \eta(x, \xi)}{\partial \xi^n} (t - \xi)^{n-\nu-1} d\xi, & \nu \in (n - 1, n), \\ \frac{\partial^n \eta(x, \xi)}{\partial \xi^n}, & \nu = n, \end{cases}$$

where n is a positive integer and $\Gamma(n - \nu)$ denotes the Gamma function.

The Laplace transform \mathcal{L} of the Caputo fractional derivative $\partial_t^\nu \eta(x, t)$ is defined as follows [6,32]:

$$\mathcal{L} \left[\partial_t^\nu \eta(x, t) \right] = s^\nu \mathcal{F}(x, s) - \sum_{m=0}^{n-1} s^{\nu-m-1} \eta^{(m)}(x, 0^+), \tag{2}$$

where $\mathcal{F}(x, s)$ denotes the Laplace transform of the function $\eta(x, t)$.

Model (1) arises in a great deal of applications, such as control theory, aerodynamics, biology, viscoelasticity, quantum mechanics, nuclear physics, etc. (see [33–42] and the references therein). For the proof regarding that Problem (1) is well posed, we refer the reader to [43,44].

The rest of this paper is structured in the following way: In Section 2, we provide the basic ideas of the q -HATM. In Section 3, we employ the q -HATM to numerically solve Problem (1), as well as provide some numerical examples to test the power and validity of this method in handling the solution of this problem. Finally, we provide some comments and conclusions in Section 4.

2. Basic Concepts of the q -HATM

Consider a general fractional PDE as follows:

$$\partial_t^\nu \eta + R\eta + \mathcal{N}\eta = \mathcal{F}(x, t), \quad n - 1 < \nu \leq n, \tag{3}$$

in which ∂_t^ν denotes the fractional Caputo derivative of order ν , R is a linear differential operator, while \mathcal{N} stands for the nonlinear one, and \mathcal{F} is a known function. Performing the Laplace transform for Equation (3) provides

$$s^\nu \mathcal{L}\{\eta\} - \sum_{j=0}^{n-1} s^{\nu-j-1} \eta^{(j)}(x, 0) + \mathcal{L}\{R\eta + \mathcal{N}\eta\} = \mathcal{L}\{\mathcal{F}\},$$

that is,

$$\mathcal{L}\{\eta\} - \frac{1}{s^\nu} \sum_{j=0}^{n-1} s^{\nu-j-1} \eta^{(j)}(x, 0) + \frac{1}{s^\nu} \mathcal{L}\{R\eta + \mathcal{N}\eta - \mathcal{F}\} = 0.$$

Then, according to the HAM method [24], a nonlinear operator $\tilde{\mathcal{N}}$ can be defined as

$$\begin{aligned} \tilde{\mathcal{N}}[\zeta(x, t; q)] &= \mathcal{L}\{\zeta(x, t; q)\} - \frac{1}{s^\nu} \sum_{j=0}^{n-1} s^{\nu-j-1} \zeta^{(j)}(x, 0; q) + \frac{1}{s^\nu} \mathcal{L}\{R\zeta(x, t; q) \\ &\quad + \mathcal{N}\zeta(x, t; q) - \mathcal{F}(x, t)\}, \end{aligned}$$

where $q \in [0, \frac{1}{n}]$, $n \geq 1$, and ζ are the real valued functions in x, t , and q . Thus, we take the zeroth-order deformation equation

$$(1 - nq) \mathcal{L}[\zeta(x, t; q) - \eta_0(x, t)] = q \hbar \mathcal{H}(x, t) \tilde{\mathcal{N}}[\zeta(x, t; q)], \tag{4}$$

where $\mathcal{H}(x, t)$ is a nonzero auxiliary function, \hbar is a non vanishing parameter (which enables one to adjust the convergence of the required series solution), $q \in [0, \frac{1}{n}]$ is an embedding parameter, \mathcal{L} denotes the Laplace transform operator, $\eta_0(x, t)$ is an initial guess for the exact solution η , and $\zeta(x, t; q)$ is an unknown function.

It is clear that when we put $q = 0$ and $q = \frac{1}{n}$ in Equation (4), it implies the following:

$$\zeta(x, t; 0) = \eta_0 \quad \text{and} \quad \zeta(x, t; \frac{1}{n}) = \eta.$$

Thus, as q deforms continuously from 0 to $\frac{1}{n}$, the function $\zeta(x, t; q)$ converges from the initial approximation $\eta_0(x, t)$ to the exact solution $\eta(x, t)$.

Now, the expansion of $\zeta(x, t; q)$ in a Taylor series with respect to q leads to

$$\zeta(x, t; q) = \eta_0(x, t) + \sum_{j=1}^{\infty} \eta_j(x, t) q^j, \tag{5}$$

where

$$\eta_j(x, t) = \frac{1}{j!} \left. \frac{\partial^j \zeta(x, t; q)}{\partial q^j} \right|_{q=0}.$$

As Liao pointed out in [26], if the parameter \hbar , the operator \mathcal{L} , the initial guess $\eta_0(x, t)$, and the auxiliary function $\mathcal{H}(x, t)$ are well chosen, then Power series (5) will converge at $q = \frac{1}{n}$ to one of the solutions of the original problem, which is given in a power series form as follows:

$$\eta(x, t) = \eta_0(x, t) + \sum_{\ell=1}^{\infty} \left(\frac{1}{n}\right)^\ell \eta_\ell(x, t).$$

In fact, these four components are presented in the zeroth deformation equation on which the success of the method relies. The choice of the operator depends on the equation to be solved, and usually it is chosen out of the operators in a problem that can be simply inverted. While the existence of the convergence control parameter \hbar distinguishes the HAM from other competent methods, it also occurs in the series solution, and it is used to adjust the convergence region. Thus, its permissible range can be predicted graphically by

using the \hbar -curves. Moreover, one has a great degree of freedom to choose its value from this range.

The function $\mathcal{H}(x, t)$ is chosen in such a way that the zeroth deformation equation produces the analytic solution as q , which deforms from 0 to $\frac{1}{\hbar}$. Finally, the initial guess can be chosen depending on the operator, as well as by the initial or boundary conditions in the problem.

Now, we differentiate the equation of the zeroth-order deformation Equation (4) k -times with respect to q , by dividing by $k!$, and by then setting $q = 0$, which produces the k th-order deformation equation

$$\mathcal{L}\{\eta_k(x, t) - \chi_k \eta_{k-1}(x, t)\} = \hbar \mathcal{H}(x, t) \tilde{\mathcal{R}}(\tilde{\eta}_{k-1}), \tag{6}$$

where

$$\tilde{\eta}_k(x, t) = [\eta_0(x, t), \eta_1(x, t), \dots, \eta_k(x, t)],$$

and

$$\tilde{\mathcal{R}}(\tilde{\eta}_{k-1}) = \frac{1}{(k-1)!} \left\{ \frac{\partial^{k-1}}{\partial q^{k-1}} \mathcal{N}[\zeta(x, t; q)] \right\} \Big|_{q=0}.$$

Next, by performing the inverse Laplace transform to Equation (6), the components $\eta_k(x, t)$ can then be determined recursively by the iterative scheme

$$\eta_k(x, t) = \chi_k \eta_{k-1}(x, t) + \hbar \mathcal{L}^{-1} \left[\mathcal{H}(x, t) \tilde{\mathcal{R}}(\tilde{\eta}_{k-1}) \right],$$

where

$$\chi_\ell = \begin{cases} 0, & \ell \leq 1, \\ n, & \ell > 1. \end{cases}$$

3. Application of the Method

The existence of the non-local integral condition in Problem (1) makes computations very complicated. Thus, to overcome this issue and to investigate the applicability and efficiency of the q -HATM for solving this problem, we transformed the integral condition in (1) to equivalent classical conditions. To this end, assume that $\int_0^1 x \eta \, dx = 0$ and $\int_0^1 x g \, dx = 0$. Then, multiply the equation

$$\partial_t^\nu \zeta - \frac{1}{x} \frac{\partial}{\partial x} \zeta - \frac{\partial^2}{\partial x^2} \zeta = g(x, t), \tag{7}$$

by x , and integrate over the interval $[0, 1]$. This implies

$$\partial_t^\nu \int_0^1 x \zeta \, dx - \int_0^1 \zeta_x \, dx - \int_0^1 x \zeta_{xx} \, dx = \int_0^1 x g \, dx,$$

or equivalently

$$\partial_t^\nu \int_0^1 x \zeta \, dx - \int_0^1 \zeta_x \, dx - \left[x \zeta_x \Big|_0^1 - \int_0^1 \zeta_x \right] = \int_0^1 x g \, dx, \tag{8}$$

which implies $\zeta_x(1, t) = 0$.

Conversely, assume that $\zeta_x(1, t) = 0$ and $\int_0^1 x g(x, t) \, dx = 0$. Again, multiply Equation (7) by x , and integrate over the interval $[0, 1]$. Then, in view of Equation (8), we conclude that $\partial_t^\nu \int_0^1 x \zeta(x, t) \, dx = 0$, which means $\int_0^1 x \zeta(x, t) \, dx = c$ for all $t \in [0, T]$, where c is a constant.

In particular we have $\int_0^1 x \zeta(x, 0) \, dx = c = 0$, since the initial condition $\zeta(x, 0) = \theta(x)$ satisfies the compatibility condition, which implies $\int_0^1 x \zeta(x, t) \, dx = 0$.

Therefore, the condition $\int_0^1 x \zeta(x, t) dx = 0$ in Problem (1) is equivalent to the conditions $\zeta_x(1, t) = 0$ and $\int_0^1 x g(x, t) dx = 0$. Hence, Problem (1) is equivalent to

$$\begin{cases} \partial_t^\nu \zeta - \frac{1}{x} \frac{\partial}{\partial x} \zeta - \frac{\partial^2}{\partial x^2} \zeta = g(x, t), 0 < \nu, x < 1, 0 < t < T, \\ \zeta(x, 0) = \theta(x), 0 < x < 1, \\ \zeta(1, t) = \psi(t), \zeta_x(1, t) = 0, 0 < t < T, \end{cases} \tag{9}$$

provided that $\int_0^1 x g(x, t) dx = 0$, where g, θ , and ψ are the given functions.

Now, in view of (2) taking a Laplace transform of both sides of the PDE in (9), this implies the following:

$$\mathcal{L}[\zeta(x, t)] - \frac{1}{s} \zeta(x, 0) - \frac{1}{s^\nu} \mathcal{L} \left[\frac{1}{x} \zeta_x(x, t) + \zeta_{xx}(x, t) + g(x, t) \right] = 0.$$

Thus, we take the operator $\tilde{\mathcal{N}}[\zeta(x, t; q)]$ as follows:

$$\begin{aligned} \tilde{\mathcal{N}}[\zeta(x, t; q)] &= \mathcal{L}\{\zeta(x, t; q)\} - \frac{1}{s} \zeta(x, 0) - \frac{1}{s^\nu} \mathcal{L}\left\{ \frac{1}{x} \frac{\partial}{\partial x} \zeta(x, t; q) \right. \\ &\quad \left. + \frac{\partial^2}{\partial x^2} \zeta(x, t; q) + g(x, t) \right\}. \end{aligned}$$

Hence, choosing the auxiliary function $\mathcal{H}(x, t) = 1$ implies that the k th-order deformation equation is given as

$$\mathcal{L}[\zeta_k(x, t) - \chi_k \zeta_{k-1}(x, t)] = \hbar \tilde{\mathcal{R}}(\vec{\zeta}_{k-1}),$$

where

$$\begin{aligned} \tilde{\mathcal{R}}(\vec{\zeta}_{k-1}) &= \mathcal{L}\{\zeta_{k-1}(x, t)\} - \left(1 - \frac{\chi_k}{n}\right) \frac{1}{s} \zeta(x, 0) - \frac{1}{s^\nu} \mathcal{L}\left\{ \frac{1}{x} \frac{\partial}{\partial x} \zeta_{k-1} \right. \\ &\quad \left. + \frac{\partial^2}{\partial x^2} \zeta_{k-1} + \left(1 - \frac{\chi_k}{n}\right) g(x, t) \right\}. \end{aligned}$$

Therefore, the successive terms of the approximate series solution can be computed recursively through the scheme

$$\zeta_k(x, t) = \chi_k \zeta_{k-1}(x, t) + \hbar \mathcal{L}^{-1} \left[\tilde{\mathcal{R}}(\vec{\zeta}_{k-1}) \right], \tag{10}$$

and the solution will be given as follows:

$$\zeta(x, t) = \zeta_0(x, t) + \sum_{i=1}^{\infty} \zeta_i(x, t).$$

Next, we test the efficiency of Scheme (10) in handling the numerical solutions of fractional problems of Type (9) by considering the following set of examples:

Example 1. Consider the homogeneous fractional order PDE

$$\partial_t^\nu \zeta - \frac{1}{x} \frac{\partial}{\partial x} \zeta - \frac{\partial^2}{\partial x^2} \zeta = 0, 0 < \nu, x < 1, 0 < t < T,$$

annexed with the conditions

$$\begin{cases} \zeta(x, 0) &= \frac{-x^2}{4} + \frac{\ln(x)}{2}, 0 < x < 1, \\ \zeta(1, t) &= -\frac{1}{4} - \frac{t^\nu}{\Gamma[\nu+1]}, \zeta_x(1, t) = 0, 0 < \nu < 1, 0 < t < T. \end{cases}$$

Solution.

Since the equation is homogeneous, it is evident that $\int_0^1 x g dx = 0$, as $g = 0$.

Now, let $\xi_0(x, t) = \zeta(x, 0) = -\frac{x^2}{4} + \frac{\ln(x)}{2}$, and since $n = 1$ in view of (10), we obtain the following:

$$\begin{aligned} \xi_1(x, t) &= \chi_1 \xi_0(x, t) + \hbar \mathcal{L}^{-1} \left[\tilde{\mathcal{R}}(\vec{\xi}_0) \right], \\ &= \hbar \mathcal{L}^{-1} \left[\tilde{\mathcal{R}}(\vec{\xi}_0) \right], \\ &= \hbar \mathcal{L}^{-1} \left[\mathcal{L}\{\xi_0(x, t)\} - \left(1 - \frac{\chi_1}{n}\right) \frac{1}{s} \zeta(x, 0) - \frac{1}{s^\nu} \mathcal{L}\left\{\frac{1}{x}(\xi_0(x, t))_x + (\xi_0(x, t))_{xx}\right\} \right], \\ &= \frac{\hbar t^\nu}{\Gamma[\nu + 1]}. \end{aligned}$$

$$\begin{aligned} \xi_2(x, t) &= \chi_2 \xi_1(x, t) + \hbar \mathcal{L}^{-1} \left[\tilde{\mathcal{R}}(\vec{\xi}_1) \right], \\ &= \xi_1(x, t) + \hbar \mathcal{L}^{-1} \left[\tilde{\mathcal{R}}(\vec{\xi}_1) \right], \\ &= \xi_1(x, t) + \hbar \mathcal{L}^{-1} \left[\mathcal{L}\{\xi_1(x, t)\} - \left(1 - \frac{\chi_2}{n}\right) \frac{1}{s} \zeta(x, 0) - \frac{1}{s^\nu} \mathcal{L}\left\{\frac{1}{x}(\xi_1(x, t))_x + (\xi_1(x, t))_{xx}\right\} \right], \\ &= (1 + \hbar) \xi_1(x, t), \\ &= (1 + \hbar) \frac{\hbar t^\nu}{\Gamma[\nu + 1]}. \end{aligned}$$

$$\begin{aligned} \xi_3(x, t) &= \chi_3 \xi_2(x, t) + \hbar \mathcal{L}^{-1} \left[\tilde{\mathcal{R}}(\vec{\xi}_2) \right], \\ &= \xi_2(x, t) + \hbar \mathcal{L}^{-1} \left[\tilde{\mathcal{R}}(\vec{\xi}_2) \right], \\ &= \xi_2(x, t) + \hbar \mathcal{L}^{-1} \left[\mathcal{L}\{\xi_2(x, t)\} - \left(1 - \frac{\chi_2}{n}\right) \frac{1}{s} \zeta(x, 0) - \frac{1}{s^\nu} \mathcal{L}\left\{\frac{1}{x}(\xi_2(x, t))_x + (\xi_2(x, t))_{xx}\right\} \right], \\ &= (1 + \hbar)^2 \frac{\hbar t^\nu}{\Gamma[\nu + 1]}. \end{aligned}$$

If we continue in this manner, we obtain

$$\xi_m(x, t) = (1 + \hbar)^{m-1} \frac{\hbar t^\nu}{\Gamma[\nu + 1]},$$

thus, the numerical solution is as follows:

$$\begin{aligned} \xi(x, t) &= \xi_0(x, t) + \sum_{i=1}^{\infty} \xi_i(x, t), \\ &= \xi_0(x, t) + (1 + \hbar) \frac{\hbar t^\nu}{\Gamma[\nu + 1]} + (1 + \hbar)^2 \frac{\hbar t^\nu}{\Gamma[\nu + 1]} + \dots, \\ &= \xi_0(x, t) + \sum_{j=1}^{\infty} (1 + \hbar)^{j-1} \frac{\hbar t^\nu}{\Gamma[\nu + 1]}, \\ &= -\frac{x^2}{4} + \frac{\ln(x)}{2} + \sum_{j=1}^{\infty} (1 + \hbar)^{j-1} \frac{\hbar t^\nu}{\Gamma[\nu + 1]}. \end{aligned} \tag{11}$$

Now, if the parameter \hbar satisfies $-2 < \hbar < 0$, then Series (11) converges, and we obtain the following series solution:

$$\begin{aligned} \xi(x, t) &= \xi_0(x, t) - \frac{t^\nu}{\Gamma[\nu + 1]}, \\ &= -\frac{x^2}{4} + \frac{\ln(x)}{2} - \frac{t^\nu}{\Gamma[\nu + 1]}. \end{aligned}$$

Let us mention that at $\nu = 1$, the last series converges to the analytical solution $\xi(x, t) = -\frac{x^2}{4} + \frac{\ln(x)}{2} - t$.

Figure 1 displays the h -curve that corresponds to the $15\hbar$ -order numerical series solution, and this shows that the values of \hbar that lead to a convergent series solution are located in the interval $(-2, 0)$.

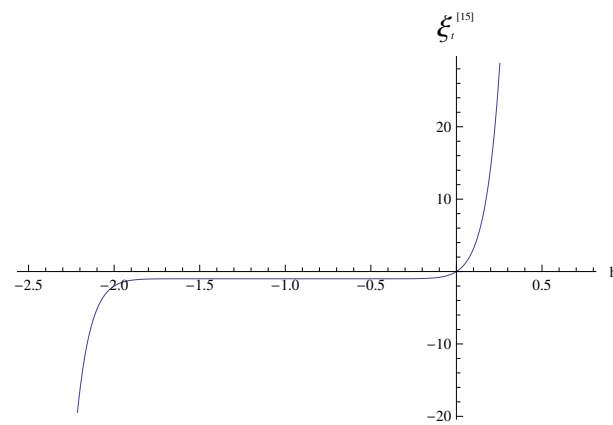


Figure 1. The \hbar -curve that corresponds to the 15th-order approximate series solution at $x = 0.75$, $t = 0$, and $\nu = 1$.

Figure 2 depicts the graphs of the truncated series solution, which used various number of terms together with the corresponding exact solution of Example 1 at $x = 0.3$, $\hbar = -0.7$, and $\nu = 0.35$. This shows that the truncated series solution of order $k = 4$ almost coincides with the analytical solution, which indicates the rapid convergence of this method.

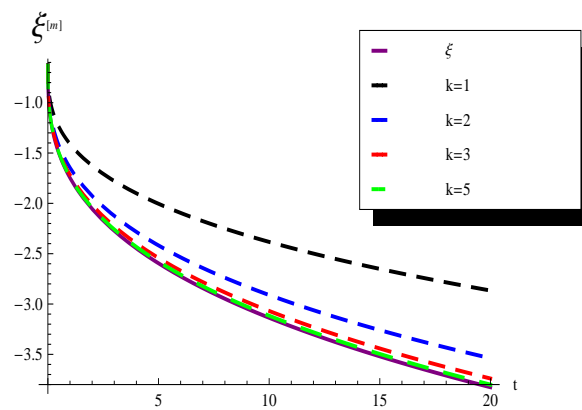


Figure 2. Truncated series solution $\zeta^{[k]}(x, t)$ at various values of k together with the analytical solution $\zeta(x, t)$ of Example 1.

In Tables 1–3, we present the numerical solutions of Example 1 that result from the k th-order truncated series solution $\zeta^{[k]}$ for the many values of k , with $\hbar = -0.7$ at various values of ν , x , and t . As we can see, the results in these tables illustrate the rapid convergences of the generated series solution, which occur just after a few terms.

Table 1. The approximate solutions of Example 1 that are generated by $\zeta^{[k]}$, and the exact solution ζ at $\nu = 0.25$ and $t = 0.1$ for certain values of x and k .

x	0.01	0.2	0.5	0.8	0.95
ζ	−2.92302	−1.43513	−1.02948	−0.891982	−0.871682
k	$\zeta^{[k]}$	$\zeta^{[k]}$	$\zeta^{[k]}$	$\zeta^{[k]}$	$\zeta^{[k]}$
1	−2.7369	−1.24901	−0.843361	−0.705859	−0.685559
2	−2.86718	−1.37929	−0.973647	−0.836145	−0.815845
3	−2.90627	−1.41838	−1.01273	−0.875231	−0.854931
13	−2.92302	−1.43513	−1.02948	−0.891982	−0.871682
100	−2.92302	−1.43513	−1.02948	−0.891982	−0.871682
200	−2.92302	−1.43513	−1.02948	−0.891982	−0.871682

Table 2. The numerical solutions of Example 1 that result from $\zeta^{[k]}$, and the exact solution ζ , at $\nu = 0.75$ and $t = 2$ for different values of x and k .

x	0.01	0.2	0.5	0.8	0.95
ζ	−4.13251	−2.64462	−2.23897	−2.10147	−2.08117
k	$\zeta^{[k]}$	$\zeta^{[k]}$	$\zeta^{[k]}$	$\zeta^{[k]}$	$\zeta^{[k]}$
1	−3.58354	−2.09565	−1.69	−1.5525	−1.5322
2	−3.96782	−2.47993	−2.07428	−1.93678	−1.91648
3	−4.0831	−2.59521	−2.18957	2.05206	−2.03176
11	−4.13251	−2.64462	−2.23897	−2.10147	−2.08117
100	−4.13251	−2.64462	−2.23897	−2.10147	−2.08117
200	−4.13251	−2.64462	−2.23897	−2.10147	−2.08117

Table 3. The numerical solutions of Example 1 that result from the truncated series $\zeta^{[m]}$, and the exact solution ζ , at $\nu = 0.9$ and $t = 10$ for various values of x and m .

x	0.01	0.2	0.5	0.8	0.95
ζ	−10.5617	−9.07378	−8.66813	−8.53063	−8.51033
m	$\zeta^{[m]}$	$\zeta^{[m]}$	$\zeta^{[m]}$	$\zeta^{[m]}$	$\zeta^{[m]}$
1	−8.08395	−6.59606	−6.19042	−6.05291	−6.03261
2	−9.81836	−8.33046	−7.92482	−7.78732	−7.76702
3	−10.3387	−8.85078	−8.44514	−8.30764	−8.28734
12	−10.5617	−9.07378	−8.66813	−8.53063	−8.51033
100	−10.5617	−9.07378	−8.66813	−8.53063	−8.51033
200	−10.5617	−9.07378	−8.66813	−8.53063	−8.51033

Table 4 shows the error resulting from the absolute difference $|\zeta(x, t) - \zeta^{[k]}(x, t)|$ of the analytical solution and the numerical truncated series solution of Example 1 for various values of x and t . It illustrates the rapid convergence of the numerical solution that is obtained by utilizing the q-HATM.

Table 4. The absolute difference between the analytical solution and the numerical solution of the order k of Example 1 at $k = 18$, $\nu = 0.3$, and $\hbar = -0.7$ for various values of x and t .

x	t				
	0.1	0.2	1	2	5
0.1	2.16353×10^{-10}	3.50633×10^{-10}	4.3168×10^{-10}	5.31461×10^{-10}	6.99606×10^{-10}
0.2	2.16353×10^{-10}	3.50633×10^{-10}	4.3168×10^{-10}	5.31461×10^{-10}	6.99606×10^{-10}
0.5	2.16353×10^{-10}	3.50633×10^{-10}	4.3168×10^{-10}	5.31461×10^{-10}	6.99606×10^{-10}
0.7	2.16353×10^{-10}	3.50633×10^{-10}	4.3168×10^{-10}	5.31461×10^{-10}	6.99606×10^{-10}
0.9	2.16353×10^{-10}	3.50633×10^{-10}	4.3168×10^{-10}	5.31461×10^{-10}	6.99606×10^{-10}

Example 2. Consider the nonhomogeneous fractional-order partial differential equation

$$\partial_t^\nu \zeta - \frac{1}{x} \frac{\partial}{\partial x} \zeta - \frac{\partial^2}{\partial x^2} \zeta = 2 - 3x, \quad 0 < \nu, \quad x < 1, \quad 0 < t < T,$$

annexed with the following conditions:

$$\begin{cases} \zeta(x, 0) = \frac{x^3}{3} - \ln(x), \quad 0 < x < 1, \\ \zeta(1, t) = \frac{1}{3} + \frac{2t^\nu}{\Gamma[\nu+1]}, \quad \zeta_x(1, t) = 0, \quad 0 < \nu < 1, \quad 0 < t < T. \end{cases}$$

Solution.

Here $g(x, t) = 2 - 3x$; hence, it is easy to check that $\int_0^1 x g dx = 0$.

Now, let $\zeta_0(x, t) = \zeta(x, 0) = \frac{x^3}{3} - \ln(x)$. Since $n = 1$ in view of (10), we obtain the following:

$$\begin{aligned} \zeta_1(x, t) &= \chi_1 \zeta_0(x, t) + \hbar \mathcal{L}^{-1} \left[\tilde{\mathcal{R}}(\vec{\zeta}_0) \right], \\ &= \hbar \mathcal{L}^{-1} \left[\tilde{\mathcal{R}}(\vec{\zeta}_0) \right], \\ &= \hbar \mathcal{L}^{-1} \left[\mathcal{L} \{ \zeta_0(x, t) \} - \left(1 - \frac{\chi_1}{n} \right) \frac{1}{s} \zeta(x, 0) - \frac{1}{s^\nu} \mathcal{L} \left\{ \frac{1}{x} (\zeta_0(x, t))_x + (\zeta_0(x, t))_{xx} \right\} \right], \\ &= -\frac{2\hbar t^\nu}{\Gamma[\nu + 1]}. \end{aligned}$$

$$\begin{aligned} \zeta_2(x, t) &= \chi_2 \zeta_1(x, t) + \hbar \mathcal{L}^{-1} \left[\tilde{\mathcal{R}}(\vec{\zeta}_1) \right], \\ &= \zeta_1(x, t) + \hbar \mathcal{L}^{-1} \left[\tilde{\mathcal{R}}(\vec{\zeta}_1) \right], \\ &= \zeta_1(x, t) + \hbar \mathcal{L}^{-1} \left[\mathcal{L} \{ \zeta_1(x, t) \} - \left(1 - \frac{\chi_2}{n} \right) \frac{1}{s} \zeta(x, 0) - \frac{1}{s^\nu} \mathcal{L} \left\{ \frac{1}{x} (\zeta_1(x, t))_x + (\zeta_1(x, t))_{xx} \right\} \right], \\ &= (1 + \hbar) \zeta_1(x, t), \\ &= -2\hbar(1 + \hbar) \frac{t^\nu}{\Gamma[\nu + 1]}. \end{aligned}$$

$$\begin{aligned} \zeta_3(x, t) &= \chi_3 \zeta_2(x, t) + \hbar \mathcal{L}^{-1} \left[\tilde{\mathcal{R}}(\vec{\zeta}_2) \right], \\ &= \zeta_2(x, t) + \hbar \mathcal{L}^{-1} \left[\tilde{\mathcal{R}}(\vec{\zeta}_2) \right], \\ &= \zeta_2(x, t) + \hbar \mathcal{L}^{-1} \left[\mathcal{L} \{ \zeta_2(x, t) \} - \left(1 - \frac{\chi_3}{n} \right) \frac{1}{s} \zeta(x, 0) - \frac{1}{s^\nu} \mathcal{L} \left\{ \frac{1}{x} (\zeta_2(x, t))_x + (\zeta_2(x, t))_{xx} \right\} \right], \\ &= -2\hbar(1 + \hbar)^2 \frac{t^\nu}{\Gamma[\nu + 1]}. \end{aligned}$$

If we continue in this manner, we obtain

$$\zeta_m(x, t) = -2\hbar(1 + \hbar)^{m-1} \frac{t^\nu}{\Gamma[\nu + 1]},$$

hence the following:

$$\begin{aligned} \zeta(x, t) &= \zeta_0(x, t) + \sum_{j=1}^{\infty} \zeta_j(x, t), \\ &= \zeta_0(x, t) - \frac{2\hbar t^\nu}{\Gamma[\nu + 1]} - (1 + \hbar) \frac{2\hbar t^\nu}{\Gamma[\nu + 1]} - (1 + \hbar)^2 \frac{2\hbar t^\nu}{\Gamma[\nu + 1]} - \dots, \\ &= \zeta_0(x, t) - \sum_{j=1}^{\infty} 2\hbar(1 + \hbar)^{j-1} \frac{t^\nu}{\Gamma[\nu + 1]}. \end{aligned} \tag{12}$$

Now, if the parameter \hbar satisfies $-2 < \hbar < 0$, then (12) converges, and we obtain the following:

$$\begin{aligned} \zeta(x, t) &= \zeta_0(x, t) + 2 \frac{t^\nu}{\Gamma[\nu + 1]}, \\ &= \frac{x^3}{3} - \ln(x) + \frac{2t^\nu}{\Gamma[\nu + 1]}. \end{aligned}$$

It is clear that at $\nu = 1$, and the last series converges to the exact solution $\zeta(x, t) = 2t + \frac{x^3}{3} - \ln(x)$.

Figure 3 displays the h -curve that corresponds to the 20th-order numerical series solution. In addition, it shows that the values of \hbar that lead to a convergent series solution are located in the interval $(-2, 0)$.

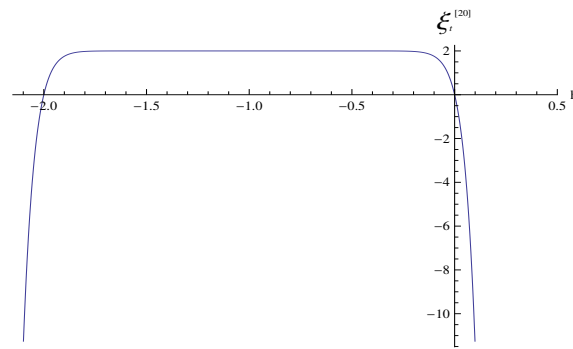


Figure 3. The h -curve that corresponds to the 20th-order approximate series solution at $x = 0.75$, $t = 0$, and $\nu = 1$.

Figure 4 depicts the graphs of the truncated series solution that use various numbers of terms together with the corresponding analytical solution of Example 2 at $x = 0.5$, $h = -0.75$, and $\nu = 0.35$. This shows that the truncated series solution of order $m = 5$ almost coincides with the analytical solution, which indicates the rapid convergence of this method.

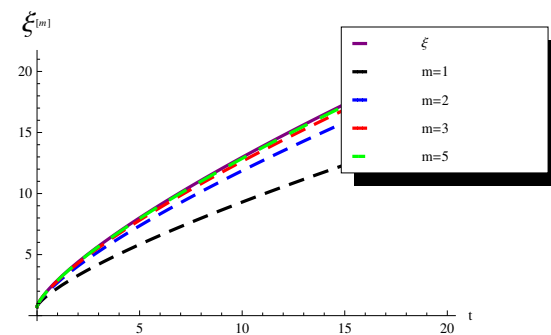


Figure 4. The truncated series solution $\zeta^{[m]}(x, t)$ with various values of m together with the analytical solution $\zeta(x, t)$ of Example 2.

In Tables 5–7, we present the approximate solutions of Example 2 that result from the k th-order series solution $\zeta^{[k]}$ for the many values of k , with $h = -0.7$ at various values of ν , x , and t . As we can see, the results in these tables illustrate the rapid convergences of the generated series solutions.

Table 5. The numerical solutions of Example 2 that were obtained using $\zeta^{[k]}$, and the exact solution ζ at $\nu = 0.25$ and $t = 0.1$ for various values of x and k .

x	0.01	0.2	0.5	0.8	0.95
ζ	5.84599	2.85292	1.97563	1.63463	1.57791
k	$\zeta^{[k]}$	$\zeta^{[k]}$	$\zeta^{[k]}$	$\zeta^{[k]}$	$\zeta^{[k]}$
1	5.47374	2.48068	1.60339	1.26238	1.20566
2	5.73432	2.74125	1.86396	1.52296	1.46623
3	5.81249	2.81942	1.94213	1.60113	1.5444
13	5.84599	2.85292	1.97563	1.63463	1.57791
100	5.84599	2.85292	1.97563	1.63463	1.57791
200	5.84599	2.85292	1.97563	1.63463	1.57791

Table 6. The approximate solutions of Example 2 that were generated by $\zeta^{[k]}$, and the exact solution ζ at $\nu = 0.75$ and $t = 2$ for different values of x and k .

x	0.01	0.2	0.5	0.8	0.95
ζ	8.26497	5.27191	4.39461	4.05361	3.99689
k	$\zeta^{[k]}$	$\zeta^{[k]}$	$\zeta^{[k]}$	$\zeta^{[k]}$	$\zeta^{[k]}$
1	7.16703	4.17397	3.29667	2.95567	2.89895
2	7.93559	4.94252	4.06523	3.72423	3.6675
3	8.16616	5.17309	4.2958	3.9548	3.89807
13	8.26497	5.2719	4.39461	4.05361	3.99689
100	8.26497	5.27191	4.39461	4.05361	3.99689
200	8.26497	5.27191	4.39461	4.05361	3.99689

Table 7. The numerical solutions of Example 2 that were produced by $\zeta^{[m]}$, and the exact solution ζ at $\nu = 0.9$ and $t = 10$ for various values of x and m .

x	0.01	0.2	0.5	0.8	0.95
ζ	21.1233	18.1302	17.2529	16.9119	16.8552
m	$\zeta^{[m]}$	$\zeta^{[m]}$	$\zeta^{[m]}$	$\zeta^{[m]}$	$\zeta^{[m]}$
1	16.1679	000	12.2975	11.9565	11.8998
2	19.6367	16.6436	15.7663	15.4253	15.3686
3	20.6773	17.6842	16.8069	16.4659	16.4092
11	21.1233	18.1302	17.2529	16.9119	16.8552
100	21.1233	18.1302	17.2529	16.9119	16.8552
200	21.1233	18.1302	17.2529	16.9119	16.8552

Table 8 shows the error that results from the absolute difference $|\zeta(x, t) - \zeta^{[k]}(x, t)|$ of the analytical solution, as well as the numerical truncated series solution of Example 1 for the various values of x and t . This illustrates the rapid convergence of the numerical solution that results from utilizing the q-HATM.

Table 8. The absolute difference between the analytical solution and the truncated series solution of order k of Example 2 at $k = 18$, $\nu = 0.6$, and $\hbar = -0.7$ for various values of x and t .

x	t				
	0.1	0.2	1	2	5
0.1	2.17826×10^{-10}	5.72127×10^{-10}	8.67183×10^{-10}	1.3144×10^{-9}	2.27768×10^{-9}
0.2	2.17827×10^{-10}	5.72126×10^{-10}	8.67183×10^{-10}	1.3144×10^{-9}	2.27768×10^{-9}
0.5	2.17826×10^{-10}	5.72127×10^{-10}	8.67182×10^{-10}	1.3144×10^{-9}	2.27768×10^{-9}
0.7	2.17826×10^{-10}	5.72127×10^{-10}	8.67182×10^{-10}	1.3144×10^{-9}	2.27768×10^{-9}
0.9	2.17827×10^{-10}	5.72127×10^{-10}	8.67182×10^{-10}	1.3144×10^{-9}	2.27768×10^{-9}

Example 3. Consider the nonhomogeneous fractional order partial differential equation:

$$\partial_t^\nu \zeta - \frac{1}{x} \frac{\partial}{\partial x} \zeta - \frac{\partial^2}{\partial x^2} \zeta = 2 - \frac{1}{x}, \quad 0 < \nu, x < 1, 0 < t < T,$$

annexed with the conditions:

$$\begin{cases} \zeta(x, 0) = 1 + x - \ln(x), & 0 < x < 1, \\ \zeta(1, t) = 1 + x + \frac{2t^\nu}{\Gamma[\nu+1]}, \zeta_x(1, t) = 0, & 0 < \nu < 1, 0 < t < T. \end{cases}$$

Solution.

Here, $g(x, t) = 2 - \frac{1}{x}$; hence, it is easy to see that $\int_0^1 x g dx = 0$.

Next, let $\xi_0(x, t) = \xi(x, 0) = 1 + x - \ln(x)$. Since $n = 1$ in view of (10), we obtain the following:

$$\begin{aligned} \xi_1(x, t) &= \chi_1 \xi_0(x, t) + \hbar \mathcal{L}^{-1} \left[\tilde{\mathcal{R}}(\vec{\xi}_0) \right], \\ &= \hbar \mathcal{L}^{-1} \left[\tilde{\mathcal{R}}(\vec{\xi}_0) \right], \\ &= \hbar \mathcal{L}^{-1} \left[\mathcal{L}\{\xi_0(x, t)\} - \left(1 - \frac{\chi_1}{n}\right) \frac{1}{s} \xi(x, 0) - \frac{1}{s^\nu} \mathcal{L}\left\{\frac{1}{x}(\xi_0(x, t))_x + (\xi_0(x, t))_{xx}\right\} \right], \\ &= -\frac{2\hbar t^\nu}{\Gamma[\nu + 1]}. \end{aligned}$$

$$\begin{aligned} \xi_2(x, t) &= \chi_2 \xi_1(x, t) + \hbar \mathcal{L}^{-1} \left[\tilde{\mathcal{R}}(\vec{\xi}_1) \right], \\ &= \xi_1(x, t) + \hbar \mathcal{L}^{-1} \left[\tilde{\mathcal{R}}(\vec{\xi}_1) \right], \\ &= \xi_1(x, t) + \hbar \mathcal{L}^{-1} \left[\mathcal{L}\{\xi_1(x, t)\} - \left(1 - \frac{\chi_2}{n}\right) \frac{1}{s} \xi(x, 0) - \frac{1}{s^\nu} \mathcal{L}\left\{\frac{1}{x}(\xi_1(x, t))_x + (\xi_1(x, t))_{xx}\right\} \right], \\ &= (1 + \hbar)\xi_1(x, t), \\ &= -2\hbar(1 + \hbar) \frac{t^\nu}{\Gamma[\nu + 1]}. \end{aligned}$$

$$\begin{aligned} \xi_3(x, t) &= \chi_3 \xi_2(x, t) + \hbar \mathcal{L}^{-1} \left[\tilde{\mathcal{R}}(\vec{\xi}_2) \right], \\ &= \xi_2(x, t) + \hbar \mathcal{L}^{-1} \left[\tilde{\mathcal{R}}(\vec{\xi}_2) \right], \\ &= \xi_2(x, t) + \hbar \mathcal{L}^{-1} \left[\mathcal{L}\{\xi_2(x, t)\} - \left(1 - \frac{\chi_3}{n}\right) \frac{1}{s} \xi(x, 0) - \frac{1}{s^\nu} \mathcal{L}\left\{\frac{1}{x}(\xi_2(x, t))_x + (\xi_2(x, t))_{xx}\right\} \right], \\ &= -2\hbar(1 + \hbar)^2 \frac{t^\nu}{\Gamma[\nu + 1]}. \end{aligned}$$

If we continue in this way we obtain

$$\xi_m(x, t) = -2\hbar(1 + \hbar)^{m-1} \frac{t^\nu}{\Gamma[\nu + 1]},$$

hence

$$\begin{aligned} \xi(x, t) &= \xi_0(x, t) + \sum_{i=1}^{\infty} \xi_i(x, t), \\ &= \xi_0(x, t) - \frac{2\hbar t^\nu}{\Gamma[\nu + 1]} - (1 + \hbar) \frac{2\hbar t^\nu}{\Gamma[\nu + 1]} - (1 + \hbar)^2 \frac{2\hbar t^\nu}{\Gamma[\nu + 1]} - \dots, \\ &= \xi_0(x, t) - \sum_{j=1}^{\infty} 2\hbar(1 + \hbar)^{j-1} \frac{t^\nu}{\Gamma[\nu + 1]}. \end{aligned} \tag{13}$$

Now, if the parameter \hbar satisfies $-2 < \hbar < 0$, then Series (13) converges, and we obtain the following:

$$\begin{aligned} \xi(x, t) &= \xi_0(x, t) + 2 \frac{t^\nu}{\Gamma[\nu + 1]}, \\ &= 1 + x - \ln(x) + \frac{2t^\nu}{\Gamma[\nu + 1]}. \end{aligned}$$

It is clear that at $\nu = 1$, the last series converges to the exact solution $\xi(x, t) = 2t + 1 + x - \ln(x)$.

Figure 5 displays the h -curve that corresponds to the 17th-order numerical series solution. Furthermore, it shows that the values of \hbar that lead to a convergent series solution are located in the interval $(-2, 0)$.

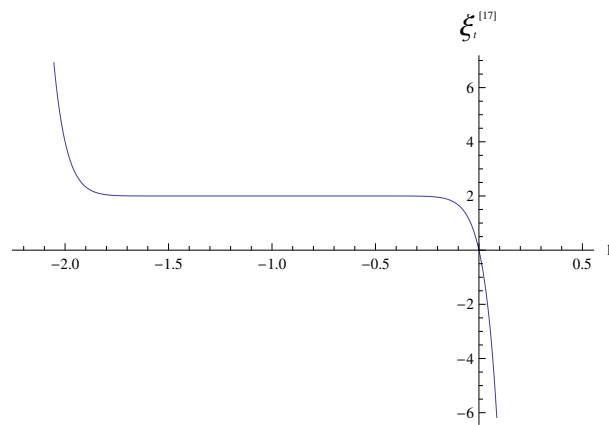


Figure 5. The \hbar -curve that corresponds to the 17th-order approximate series solution at $x = 0.75, t = 0,$ and $\nu = 1.$

Figure 6 depicts the graphs of the truncated series solution that use various numbers of terms together with the corresponding exact solution of Example 3 at $x = 0.8, \hbar = -0.7,$ and $\nu = 0.6.$ This shows that the truncated series solution of order $m = 5$ almost coincides with the analytical solution, which indicates the rapid convergence of this method.

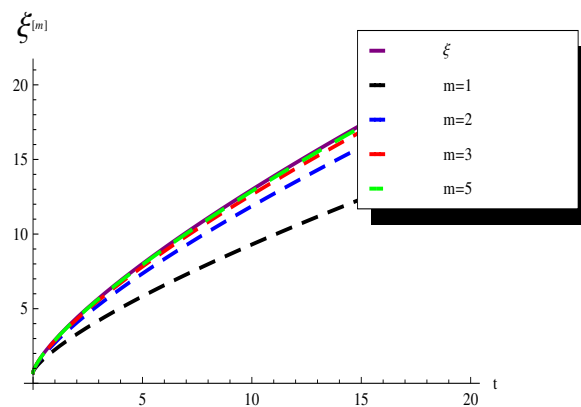


Figure 6. Truncated series solution $\zeta^{[m]}(x, t)$ with various values of m together with the exact solution $\zeta(x, t)$ of Example 3.

In Tables 9–11, we present the approximate solutions of Example 3 that are produced by an m^{th} -order series solution $\zeta^{[m]}$ for many values of m with $\hbar = -0.7,$ which is achieved by using various values of $\nu, x,$ and $t.$ As we can see, the results in these tables illustrate the rapid convergences of the generated series solutions.

Table 9. The approximate solutions of Example 3 that were generated by $\zeta^{[m]},$ and the exact solution ζ at $\nu = 0.25$ and $t = 0.1$ for various values of x and $m.$

x	0.01	0.2	0.5	0.8	0.95
ζ	6.85599	4.05026	3.43397	3.26396	3.24211
m	$\zeta^{[m]}$	$\zeta^{[m]}$	$\zeta^{[m]}$	$\zeta^{[m]}$	$\zeta^{[m]}$
1	6.48374	3.67801	3.06172	2.89172	2.86987
2	6.74432	3.93858	3.32229	3.15229	3.13044
3	6.82249	4.01676	3.40047	3.23046	3.20861
11	6.85599	4.05026	3.43397	3.26396	3.24211
100	6.85599	4.05026	3.43397	3.26396	3.24211
200	6.85599	4.05026	3.43397	3.26396	3.24211

Table 10. The approximate solutions of Example 3 that are generated by $\zeta^{[m]}$, and the exact solution ζ , at $\nu = 0.75$ and $t = 2$ for various values of x and m .

x	0.01	0.2	0.5	0.8	0.95
ζ	9.27497	6.46924	5.85295	5.68294	5.66109
m	$\zeta^{[m]}$	$\zeta^{[m]}$	$\zeta^{[m]}$	$\zeta^{[m]}$	$\zeta^{[m]}$
1	8.17703	5.3713	4.75501	4.585	4.56315
2	8.94559	6.13986	5.52357	5.35356	5.33171
3	9.17616	6.37042	5.75413	5.58413	5.56228
12	9.27497	6.46924	5.85295	5.68294	5.66109
100	9.27497	6.46924	5.85295	5.68294	5.66109
200	9.27497	6.46924	5.85295	5.68294	5.66109

Table 11. The approximate solutions of Example 3 that are generated by $\zeta^{[m]}$, and the exact solution ζ at $\nu = 0.9$ and $t = 10$ for various values of x and m .

x	0.01	0.2	0.5	0.8	0.95
ζ	22.1333	19.3276	18.7113	18.5413	18.5194
m	$\zeta^{[m]}$	$\zeta^{[m]}$	$\zeta^{[m]}$	$\zeta^{[m]}$	$\zeta^{[m]}$
1	17.1779	14.3721	13.7558	13.5858	13.564
2	20.6467	17.8409	17.2246	17.0546	17.0328
3	21.6873	18.8816	18.2653	18.0953	18.0734
12	22.1333	19.3276	18.7113	18.5413	18.5194
100	22.1333	19.3276	18.7113	18.5413	18.5194
200	22.1333	19.3276	18.7113	18.5413	18.5194

Table 12 shows the error that results from the absolute difference $|\zeta(x, t) - \zeta^{[k]}(x, t)|$ of the analytical solution, as well as the numerical truncated series solution of Example 1 for various values of x and t . It illustrates the rapid convergence of the numerical solution that results from utilizing the q -HATM.

Table 12. The absolute difference between the analytical solution and the truncated series solution of order k of Example 3 at $k = 19$, $\nu = 0.75$, and $\hbar = -0.7$ for various values of x and t .

x	t				
	0.1	0.2	1	2	5
0.1	4.49769×10^{-11}	1.5039×10^{-10}	2.52923×10^{-10}	4.25363×10^{-10}	8.457×10^{-10}
0.2	4.49769×10^{-11}	1.5039×10^{-10}	2.52923×10^{-10}	4.25365×10^{-10}	8.45699×10^{-10}
0.5	4.49765×10^{-11}	1.50389×10^{-10}	2.52924×10^{-10}	4.25364×10^{-10}	8.45699×10^{-10}
0.7	4.49769×10^{-11}	1.50389×10^{-10}	2.52923×10^{-10}	4.25365×10^{-10}	8.457×10^{-10}
0.9	4.49769×10^{-11}	1.50389×10^{-10}	2.52922×10^{-10}	4.25364×10^{-10}	8.45699×10^{-10}

4. Conclusions

In this article, a numerical solution of a fractional order IBVP with a non-local constraint is obtained via the q -HATM. Several examples are given to illustrate the efficiency of the derived iterative scheme. The exact solution is obtained for each one of these examples. The convergence of the numerical solutions of these examples was studied both numerically and graphically. A comparison of the analytical and numerical solution was conducted using the absolute error for the different values of x and t , as in Tables 4, 8, and 12. Also, a graphical comparison of the truncated series solution with various number of terms and the exact solution is illustrated in Figures 2, 4, and 6. These results show that the q -HATM is an efficient method for solving these types of singular non-local fractional partial differential equations.

Author Contributions: Conceptualization, S.M.; methodology, S.M. and H.A.; software, S.M. and H.A.; validation, S.M. and H.A.; formal analysis, S.M. and H.A.; resources, S.M. and H.A.; investigation, S.M. and H.A. All authors have read and agreed to the published version of the manuscript.

Funding: The authors would like to extend their sincere appreciation to Researchers Supporting Project number (RSP2023R472 King Saud University, Riyadh, Saudi Arabia).

Data Availability Statement: Not applicable.

Acknowledgments: The authors would like to extend their sincere appreciation to Researchers Supporting Project number (RSP2023R472 King Saud University, Riyadh, Saudi Arabia).

Conflicts of Interest: All authors declare no conflict of interest in this paper.

References

1. Du, M.; Wang, Z.; Hu, H. Measuring memory with the order of fractional derivative. *Sci. Rep.* **2013**, *3*, 3431.
2. Scalar, E.; Gorenflo, R.; Mainardi, F. Fractional calculus and continuous time finance. *Physica A* **2000**, *284*, 376–384.
3. West, B.J.; Turalskal, M.; Grigolini, P. Fractional calculus ties the microscopic and macroscopic scales of complex network dynamics. *New J. Phys.* **2015**, *17*, 45009.
4. Tarasov, V.E. Fractional vector calculus and fractional Maxwell's equations. *Ann. Phys.* **2008**, *323*, 2756–2778.
5. Oldham, K.B.; Spanier, J. *The Fractional Calculus*; Academic Press: New York, NY, USA, 1974.
6. Miller, K.S.; Ross, B. *An Introduction to the Fractional Calculus and Fractional Differential Equations*; Wiley: New York, NY, USA, 1993.
7. Podlubny, I. *Fractional Differential Equations*; Academic Press: San Diego, CA, USA, 1999; Volume 198.
8. Kilbas, A.A.; Srivastava, H.M.; Trujillo, J.J. *Theory and Applications of Fractional Differential Equations*; Elsevier: Amsterdam, The Netherlands, 2006; Volume 204.
9. Baleanu, D.; Diethelm, K.; Scalas, E.; Trujillo, J.J. *Fractional Calculus Models and Numerical Methods*; World Scientific: Singapore, 2012.
10. Kumar, S. A numerical study for solution of time fractional nonlinear shallow-water equation in oceans. *Z. Naturforsch. A* **2013**, *68*, 547–553.
11. Agarwal, R.P.; Benchohra, M.; Hamani, S. A survey on existence results for boundary value problems of nonlinear fractional differential equations and inclusions. *Acta Appl. Math.* **2010**, *109*, 973–1033.
12. Kumar, D.; Singh, J.; Kumar, S. Analytical modeling for fractional multi-dimensional diffusion equations by using Laplace transform. *Commun. Numer. Anal.* **2015**, *1*, 16–29.
13. Dehghan, M.; Shakeri, F. A semi-numerical technique for solving the multi-point boundary value problems and engineering applications. *Int. J. Numer. Methods Heat Fluid Flow* **2011**, *21*, 794–809.
14. Saadatmandi, A.; Dehghan, M. A new operational matrix for solving fractional-order differential equations. *Comput. Math. Appl.* **2010**, *59*, 1326–1336.
15. Saadatmandi, A.; Dehghan, M. A tau approach for solution of the space fractional diffusion equation. *Comput. Math. Appl.* **2011**, *62*, 1135–1142.
16. Jafari, H.; Golbabai, A.; Seifi, S.; Sayevand, K. Homotopy analysis method for solving multi-term linear and nonlinear diffusion wave equations of fractional order. *Comput. Math. Appl.* **2010**, *66*, 838–843.
17. Veerasha, P.; Prakasha, D.G.; Baskonus, H.M. Novel simulations to the time-fractional Fisher's equation. *Math. Sci.* **2019**, *13*, 33–42. [[CrossRef](#)]
18. Mark, M. Meerschaerta and Charles Tadjeran, Finite difference approximations for two-sided space-fractional partial differential equations. *Appl. Numer. Math.* **2006**, *56*, 80–90.
19. Jianga, Y.; Ma, J. High-order finite element methods for time-fractional partial differential equations. *J. Comput. Appl. Math.* **2011**, *235*, 3285–3290. [[CrossRef](#)]
20. Odibat, Z.; Momani, S. The variational iteration method: An efficient scheme for handling fractional partial differential equations in fluid mechanics. *Comput. Math. Appl.* **2009**, *58*, 2199–2208.
21. Momani, S.; Odibat, Z. Analytical solution of a time-fractional Navier-Stokes equation by Adomian decomposition method. *Appl. Math. Comput.* **2006**, *177*, 488–494.
22. El-Tawil, M.A.; Huseen, S.N. The q-homotopy analysis method (q-HAM). *Int. J. Appl. Math. Mech.* **2012**, *8*, 51–75.
23. El-Tawil, M.A.; Huseen, S.N. On convergence of the qhomotopy analysis method. *Int. J. Contemp. Math. Sci.* **2013**, *8*, 481–497. [[CrossRef](#)]
24. Liao, S.J. The Proposed Homotopy Analysis Technique for the Solution of Nonlinear Problems. Ph.D. Thesis, Shanghai Jiao Tong University, Shanghai, China, 1992.
25. Liao, S.J. Homotopy analysis method a new analytical technique for nonlinear problems. *Commun. Nonl. Sci. Numer. Simul.* **1997**, *2*, 95–100.
26. Liao, S.J. *Beyond Perturbation: Introduction to the Homotopy Analysis Method*; Chapman and Hall/CRC Press: Boca Raton, FL, USA, 2003.

27. Xu, D.L.; Lin, Z.L.; Liao, S.J.; Stiasnie, M. On the steady-state fully resonant progressive waves in water of finite depth. *J. Fluid. Mech.* **2012**, *710*, 379–418.
28. Liao, S.J. On the homotopy analysis method for nonlinear problems. *Appl. Math. Comput.* **2004**, *147*, 499–513.
29. Prakash, A.; Kaur, H. q-homotopy analysis transform method for space and time-fractional KdV-Burgers equation. *Nonlinear Sci. Lett. A* **2018**, *9*, 44–61.
30. Arafa, A.A.M.; Hagag, A.M.S. q-homotopy analysis transform method applied to fractional Kundu-Eckhaus equation and fractional massive Thirring model arising in quantum field theory. *Asian-Eur. J. Math.* **2019**, *12*, 1793–5571. [[CrossRef](#)]
31. Kumar, D.; Singh, J.; Baleanu, D. A new analysis for fractional model of regularized long-wave equation arising in ion acoustic plasma waves. *Math. Methods Appl. Sci.* **2017**, *40*, 5642–5653
32. Caputo, M. *Elasticità e Dissipazione*; Zanichelli: Bologna, Italy, 1969.
33. Bagley, R.L.; Torvik, P.J. A theoretical basis for the application of fractional calculus to viscoelasticity. *J. Rheol.* **1983**, *27*, 201–210.
34. Sorrentinos, G. Fractional derivative linear models for describing the viscoelastic dynamic behavior of polymeric beams. In Proceedings of the IMAS, Saint Louis, MO, USA, 30 January–2 February 2006.
35. Mainardi, F. *Fractional Calculus and Waves in linear Viscoelasticity: An Introduction to Mathematical Models*; World Scientific: Singapore, 2010.
36. Goloviznin, V.M.; Kisilev, V.P.; Korotkin, I.A.; Yurkov, Y.I. Direct Problems of Nonclassical Radionuclide Transfer in Geological Formations. *Izv. Ross. Akad. Nauk Energ.* **2004**, *4*, 121–130.
37. Chukbar, K.V. The Stochastic Transfer and Fractional Derivatives. *Zh. Eksp. Teor. Fiz.* **1995**, *108*, 1875–1884.
38. Sabatier, J.; Agrawal, O.P.; Machado, J.A.T. (Eds.) *Advances in Fractional Calculus: Theoretical Developments and Applications in Physics and Engineering*; Springer: Dordrecht, The Netherlands, 2007.
39. Benchohra, M.; Hamani, S.; Ntouyas, S.K. Boundary value problems for differential equations with fractional order and nonlocal conditions. *Nonlinear Anal.* **2009**, *71*, 2391–2396.
40. Lazarevic, M.P.; Spasic, A.M. Finite-time stability analysis of fractional order time-delay systems: Gronwall’s approach. *Math. Comput. Model.* **2009**, *49*, 475–481.
41. Nieto, J.J. Maximum principles for fractional differential equations derived from Mittag-Leffler functions. *Appl. Math. Lett.* **2010**, *23*, 1248–1251.
42. Zhang, S.Q. Positive solutions to singular boundary value problem for nonlinear fractional differential equation. *Comput. Math. Appl.* **2010**, *59*, 1300–1309.
43. Mesloub, S.; Obaidat, S. Homotopy Analysis Method for a Fractional Order Equation with Dirichlet and Non-Local Integral Conditions. *Mathematics* **2019**, *7*, 1167. [[CrossRef](#)]
44. Mesloub, S.; Bachar, I. On a nonlocal 1-D initial value problem for a singular fractional-order parabolic equation with Bessel operator. *Adv. Differ. Equ.* **2019**, *2019*, 254. [[CrossRef](#)]

Disclaimer/Publisher’s Note: The statements, opinions and data contained in all publications are solely those of the individual author(s) and contributor(s) and not of MDPI and/or the editor(s). MDPI and/or the editor(s) disclaim responsibility for any injury to people or property resulting from any ideas, methods, instructions or products referred to in the content.